PROCEEDINGS OF SCIENCE

A Comprehensive Study of Double pion Photoproduction: A Regge Approach

Nadine Hammoud,[a,*] **Łukasz Bibrzycki,**[b] **Vincent Mathieu,**[a,c] **Robert J. Perry**[a] **and Adam P. Szczepaniak**[d,e,f]

[a]*Departament de Física Quàntica i Astrofísica and Institut de Ciències del Cosmos, Universitat de Barcelona,*
E-08028 Barcelona, Spain.

[b]*AGH University of Krakow, Faculty of Physics and Applied Computer Science,*
al. Mickiewicza 30, PL-30059 Kraków, Poland

[c]*Departamento de Física Teórica, Universidad Complutense de Madrid and IPARCOS,*
E-28040 Madrid, Spain

[d]*Theory Center, Thomas Jefferson National Accelerator Facility,*
Newport News, VA 23606, USA

[e]*Center for Exploration of Energy and Matter, Indiana University,*
Bloomington, IN 47403, USA

[f]*Department of Physics, Indiana University,*
Bloomington, IN 47405, USA

E-mail: nhammoud@icc.ub.edu

Presented here is a theoretical model designed to investigate double pion photoproduction, within the photon energy range of 3.0 to 3.8 GeV and momentum transfer range of $0.4 < -t < 1.0$ GeV^2. This model integrates contributions from resonances such as the $\rho(770)$, as well as the primary background from the Deck mechanism. Utilizing the Regge formalism and incorporating the established Deck mechanism, the model emphasizes the significance of the $\rho(770)$ resonance, highlighting its role in representing P-wave contributions arising from pomeron alongside other exchanges. However, at high momentum transfers, indications of s-channel helicity non-conservation emerge, suggesting the involvement of additional partial waves, notably the S and D waves. The model is further extended to include scalar mesons such as $f_0(500)$, $f_0(980)$, and $f_0(1370)$, along with the tensor meson $f_2(1270)$, influencing S- and D-wave effects, respectively. Predictions of angular moments are compared with CLAS data, and the analysis further explores the t-dependence of the Regge amplitude residue function for subdominant exchanges.

10th International Conference on Quarks and Nuclear Physics (QNP2024)
8-12 July, 2024
Barcelona, Spain

*Speaker

PoS(QNP2024)041

1. Introduction

Two-pion photoproduction has been widely studied in hadron spectroscopy to probe light meson resonances. Due to the absence of free pion targets, photoproduction serves as a crucial tool for such investigations. Recent developments in the field, particularly with high-precision data, necessitate sophisticated amplitude analysis methods. Regge theory provides a useful framework in the high-energy, small momentum transfer limit, where the scattering amplitude is dominated by Pomeron exchange [1, 2]. The study of two-pion final states, especially in the region dominated by the $\rho(770)$ resonance, reveals key features such as s-channel helicity conservation (SCHC) [3] and the deformation of the $\rho(770)$ lineshape [4–6]. While simple Pomeron models describe the data at small momentum transfer ($|t| \lesssim 0.4$ GeV^2) [7], additional exchanges are necessary to capture the behavior at larger $|t|$ [8]. This motivates the development of more detailed models, especially as higher precision measurements become available [9].

2. Kinematics and Angular Moments

We consider the reaction:

$$\gamma(q, \lambda_\gamma) + p(p_1, \lambda_1) \to \pi^+(k_1) + \pi^-(k_2) + p(p_2, \lambda_2), \tag{1}$$

where the helicities are defined in the $\pi^+\pi^-$ helicity frame, with $\mathbf{k}_1^{\mathrm{H}} = -\mathbf{k}_2^{\mathrm{H}}$ and $\mathbf{p}_2^{\mathrm{H}}$ setting the negative z-axis. The plane of the reaction defines the x-z plane, and the y-axis is perpendicular, aligned with $\mathbf{p}_2^{\mathrm{H}} \times \mathbf{q}^{\mathrm{H}}$. The angles of the π^+ are denoted by $\Omega^{\mathrm{H}} = (\theta^{\mathrm{H}}, \phi^{\mathrm{H}})$. The helicity amplitudes of this $2 \to 3$ process depend on five kinematic variables: the π^+ angles and the invariants s, t, and s_{12}:

$$s = (p_1 + q)^2, \quad t = (p_1 - p_2)^2, \quad s_{12} = (k_1 + k_2)^2.$$

The differential cross section is:

$$\frac{d\sigma}{dt\, d\sqrt{s_{12}}\, d\Omega^{\mathrm{H}}} = \kappa \sum_{\lambda_1 \lambda_\gamma \lambda_2} |\mathcal{M}_{\lambda_\gamma \lambda_1 \lambda_2}(s, t, s_{12}, \Omega^{\mathrm{H}})|^2, \tag{2}$$

where κ contains kinematic factors, including the Källén function $\lambda(a, b, c)$. Angular moments are defined as:

$$\langle Y_M^L \rangle = \sqrt{4\pi} \int d\Omega^{\mathrm{H}} \frac{d\sigma}{dt\, d\sqrt{s_{12}}\, d\Omega^{\mathrm{H}}} \mathrm{Re}[Y_M^L(\Omega^{\mathrm{H}})], \tag{3}$$

and the partial-wave expansion of the amplitude is:

$$\mathcal{M}_{\lambda_\gamma \lambda_1 \lambda_2}(s, t, s_{12}, \Omega^{\mathrm{H}}) = \sum_{lm} \mathcal{M}^l_{\lambda_\gamma \lambda_1 \lambda_2 m}(s, t, s_{12}) Y_m^l(\Omega^{\mathrm{H}}). \tag{4}$$

Parity relations reduce the number of independent helicity amplitudes, and partial waves are labeled using spectroscopic notation such as S, P, D, etc.

PoS(QNP2024)041

3. The Model

This study investigates the angular moments of the $\pi^+\pi^-$ system, focusing on low-energy resonances decaying into $\pi^+\pi^-$. The resonances are modeled as a two-step process: t-channel scattering between the nucleon and photon, followed by decay into the two-pion final state. Key resonances include the $\rho(770)$ at $\sqrt{s_{12}} \sim 0.77$ GeV, alongside $f_0(500)$, $f_0(980)$, $f_0(1370)$, and $f_2(1270)$. The primary background arises from the Deck mechanism, where a photon produces a pion pair, leading to one-pion exchange. The total amplitude is expressed as:

$$\mathcal{M}_{\lambda_\gamma\lambda_1\lambda_2}(s,t,s_{12},\Omega^{\mathrm{H}}) = \mathcal{M}^{\mathrm{R}}_{\lambda_\gamma\lambda_1\lambda_2}(s,t,s_{12},\Omega^{\mathrm{H}}) + \mathcal{M}^{\mathrm{NR}}_{\lambda_\gamma\lambda_1\lambda_2}(s,t,s_{12},\Omega^{\mathrm{H}}), \tag{5}$$

where the first term is the resonant contribution and the second is the nonresonant component.

3.1 Resonant Amplitude

The resonant amplitude is written as a sum of individual resonances:

$$\mathcal{M}^{\mathrm{R}}_{\lambda_\gamma\lambda_1\lambda_2}(s,t,s_{12},\Omega^{\mathrm{H}}) = \sum_{\mathcal{R}} \mathcal{M}^{\mathcal{R}}_{\lambda_\gamma\lambda_1\lambda_2}(s,t,s_{12},\Omega^{\mathrm{H}}), \tag{6}$$

where the sum runs over resonances . Each resonance amplitude is decomposed into a production term (formation of a resonance $\mathcal{R}$ with spin J) and a decay term (resonance decay to two pions):

$$\mathcal{M}^{\mathcal{R}}_{\lambda_\gamma\lambda_1\lambda_2}(s,t,s_{12},\Omega^{\mathrm{H}}) = \sum_{M=-J}^{J} \mathcal{M}^{\gamma p\to\mathcal{R}p}_{\lambda_\gamma\lambda_1 M\lambda_2}(s,t) A^{\mathcal{R}}(s_{12}) Y^J_M(\Omega^{\mathrm{H}}). \tag{7}$$

The two-pion mass dependence is assumed to come from $A^{\mathcal{R}}(s_{12})$, modeled as a Breit-Wigner distribution, though more sophisticated treatments exist in the literature.

3.1.1 Production Amplitude

The production amplitude for $\gamma p \to \mathcal{R}p$ at high energies is modeled using Regge theory, leading to expressions for t-channel exchange amplitudes:

$$\mathcal{M}^{\mathrm{E}}_{\lambda_\gamma\lambda_1 M\lambda_2}(s,t) = \sum_j \mathcal{T}^{\alpha_1\cdots\alpha_j}_{\lambda_\gamma M} \mathcal{P}^{\mathrm{E}}_{\alpha_1\cdots\alpha_j;\beta_1\cdots\beta_j} \mathcal{B}^{\beta_1\cdots\beta_j}_{\lambda_1\lambda_2}. \tag{8}$$

At high energies and low t, the amplitude matches Born-term t-channel diagrams, with the Regge pole propagator given by:

$$R^{\mathrm{E}}(s,t) = \frac{1}{s_0}\frac{\alpha^{\mathrm{E}}(t)}{\alpha^{\mathrm{E}}(0)}\frac{1+\tau^{\mathrm{E}}e^{-i\pi\alpha^{\mathrm{E}}(t)}}{\sin\pi\alpha^{\mathrm{E}}(t)}\left(\frac{s}{s_0}\right)^{\alpha^{\mathrm{E}}(t)-1}. \tag{9}$$

Here, $\alpha^{\mathrm{E}}(t)$ is the Regge trajectory, and s_0 is set to 1 GeV^2. The helicity-dependent coupling of the Reggeon to the photon and nucleon is expressed as:

$$\mathcal{T}\times\mathcal{B} \to \mathcal{T}^{\alpha}_{\lambda_\gamma,M}\bar{u}_{\lambda_2}(p_2)\gamma_\alpha u_{\lambda_1}(p_1), \tag{10}$$

where $\mathcal{T}$ is the top vertex and $\mathcal{B}$ is the bottom vertex.

PoS(QNP2024)041

3.2 Nonresonant Amplitude

In addition to modeling the leading resonant contributions, the model incorporates the expected background from the Deck process. To improve the description of the angular moments, empirically-motivated polynomial backgrounds are added to the low-lying partial waves. The nonresonant model can be written as:

$$\mathcal{M}^{\mathrm{NR}}_{\lambda_\gamma\lambda_1\lambda_2}(s,t,s_{12},\Omega^{\mathrm{H}}) = \mathcal{M}^{\mathrm{Deck}}_{\lambda_\gamma\lambda_1\lambda_2}(s,t,s_{12},\Omega^{\mathrm{H}}) + \mathcal{M}^{\mathrm{empir.}}_{\lambda_\gamma\lambda_1\lambda_2}(s,t,s_{12},\Omega^{\mathrm{H}}). \tag{11}$$

3.2.1 Deck Mechanism

The Deck mechanism operates as a sequential process in which a single off-shell pion, produced by photon decay, elastically recoils against the nucleon target, resulting in the final state $p\pi^+\pi^-$. The gauge-invariant Deck Model amplitude, as formulated in [10, 11], is expressed as:

$$\begin{aligned}\mathcal{M}^{\mathrm{GI\,Deck}}_{\lambda_1\lambda_2\lambda_\gamma}(s,t,s_{\pi\pi},\Omega) = \sqrt{4\pi\alpha}\Bigg[&\left(\frac{\epsilon(q,\lambda_\gamma)\cdot k_1}{q\cdot k_1} - \frac{\epsilon(q,\lambda_\gamma)\cdot(p_1+p_2)}{q\cdot(p_1+p_2)}\right)\beta(u_1)M^-_{\lambda_1\lambda_2}(s_2,t;u_1)\\ &-\left(\frac{\epsilon(q,\lambda_\gamma)\cdot k_2}{q\cdot k_2} - \frac{\epsilon(q,\lambda_\gamma)\cdot(p_1+p_2)}{q\cdot(p_1+p_2)}\right)\beta(u_2)M^+_{\lambda_1\lambda_2}(s_1,t;u_2)\Bigg],\end{aligned} \tag{12}$$

where $\beta(u_i) = \exp\left(\frac{u_i - u_i^{\min}}{\Lambda_\pi^2}\right)$ acts as a form factor, suppressing the pion propagator for one-pion exchange at large u_i with $\Lambda_\pi = 0.9$ GeV. The term $M^{\pm}_{\lambda_1\lambda_2}$ represents the scattering amplitudes for $p + \pi^{*\pm} \longrightarrow p + \pi^{\pm}$.

3.2.2 Polynomial Backgrounds

Empirically, it is found that the Deck mechanism alone cannot describe the entire nonresonant background. Therefore, an empirical polynomial background is added to the low-lying partial waves. For $J = 0, 1$, an additional amplitude with the same structure as the resonant amplitude is included, where the function $A^J(s_{12})$ is taken as a polynomial:

$$A^J(s_{12}) = (s_{12} - s_{12}^{\min})(s_{12} - s_{12}^{\max}), \tag{13}$$

with:

$$s_{12}^{\min} = 4m_\pi^2, \tag{14}$$

$$s_{12}^{\max} = s + m_p^2 - \frac{1}{2m_p^2}\left[(s+m_p^2)(2m_p^2 - t) - \lambda^{1/2}(s,m_p^2,0)\lambda^{1/2}(t,m_p^2,m_p^2)\right]. \tag{15}$$

The constants $s_{12}^{\min}$ and $s_{12}^{\max}$ are chosen to avoid an unnaturally large nonresonant contribution near the threshold. The couplings $b_M^{\mathrm{E},J}$ are determined empirically.

4. Results

The model consists of 30 free parameters, $\{a_M^{\mathrm{E},\mathcal{R}}, b_M^{\mathrm{E},J}\}$, which determine the relative strengths and phases of the production mechanisms. These parameters are fitted to the angular moments

PoS(QNP2024)041

$\langle Y_L^M \rangle$ measured by CLAS at photon laboratory energies ranging from 3.0 to 3.8 GeV, with a focus on the highest energy bin (E_γ = 3.6–3.8 GeV) and evaluated at E_γ = 3.7 GeV, aligning with the Regge approach's suitability for high energies. The results include fits for angular moments with $L = 0, 1, 2$ and $M = 0, \ldots, L$. The t-dependence of the nonresonant Deck amplitude and the Pomeron-mediated ρ photoproduction components is not fitted. We adopt a "bottom-up" approach [12], fitting each t bin separately to allow the data to determine the t-dependence, with each fit based on 600 data points. Due to space constraints, we present fitting results for only one t bin, specifically at $t = -0.45$ GeV^2, in Fig. [1].

4.1 Discussion

The model reveals a slight increase in uncertainty around masses near 1.4 GeV, where D-wave contributions are expected to dominate, particularly due to the presence of the $f_2(1270)$ resonance. The only other D-wave contribution comes from the Deck amplitude, which is fully constrained and lacks free parameters. As noted in [10], the Deck mechanism's D-wave contribution is significantly smaller than that of the P-wave, resulting in minimal interference among resonant D-wave helicity amplitudes and, consequently, less constrained relative strengths and phases.

Despite the model's overall good agreement with the data, several discrepancies are observed. Specifically, the model predicts a shallower dip in the $\sqrt{s_{12}}$ values around the $\rho(770)$ mass and for momentum transfers $|t| \in [0.45, 0.75]$ GeV^2 in the $\langle Y_0^1 \rangle$ moment compared to experimental results. Additionally, the fitted $\langle Y_1^1 \rangle$ moment exhibits slight phase discrepancies with the data, as shown in Fig. [1].

These discrepancies may stem from the modeling of the nucleon-reggeon vertex, defined as $\mathcal{B}^\alpha_{\lambda_1\lambda_2} = \overline{u}_{\lambda_2}(p_2)\gamma^\alpha u_{\lambda_1}(p_1)$, which may not reflect the most general form. This limitation could lead the model to impose relationships between helicity amplitudes that lack a solid physical foundation. Unfortunately, further investigation is hindered by the current lack of experimental access to individual nucleon helicity couplings.

References

[1] T. Regge. Introduction to complex orbital momenta. *Nuovo Cim.*, 14:951, 1959.

[2] A. C. Irving and R. P. Worden. Regge Phenomenology. *Phys. Rept.*, 34:117–231, 1977.

[3] Joseph Ballam et al. CONSERVATION OF S CHANNEL HELICITY IN rho0 PHOTOPRODUCTION. *Phys. Rev. Lett.*, 24:960–963, 1970. [Erratum: Phys. Rev. Lett. 24, 1967 (1970)].

[4] S. D. Drell. Peripheral Contributions to High-Energy Interaction Processes. *Rev. Mod. Phys.*, 33:458–466, 1961.

[5] P. Soding. On the Apparent shift of the rho meson mass in photoproduction. *Phys. Lett.*, 19:702–704, 1966.

[6] Theodore Bauer. Anomalous real parts in the t matrices of unstable particles. *Phys. Rev. Lett.*, 25:485–488, Aug 1970.

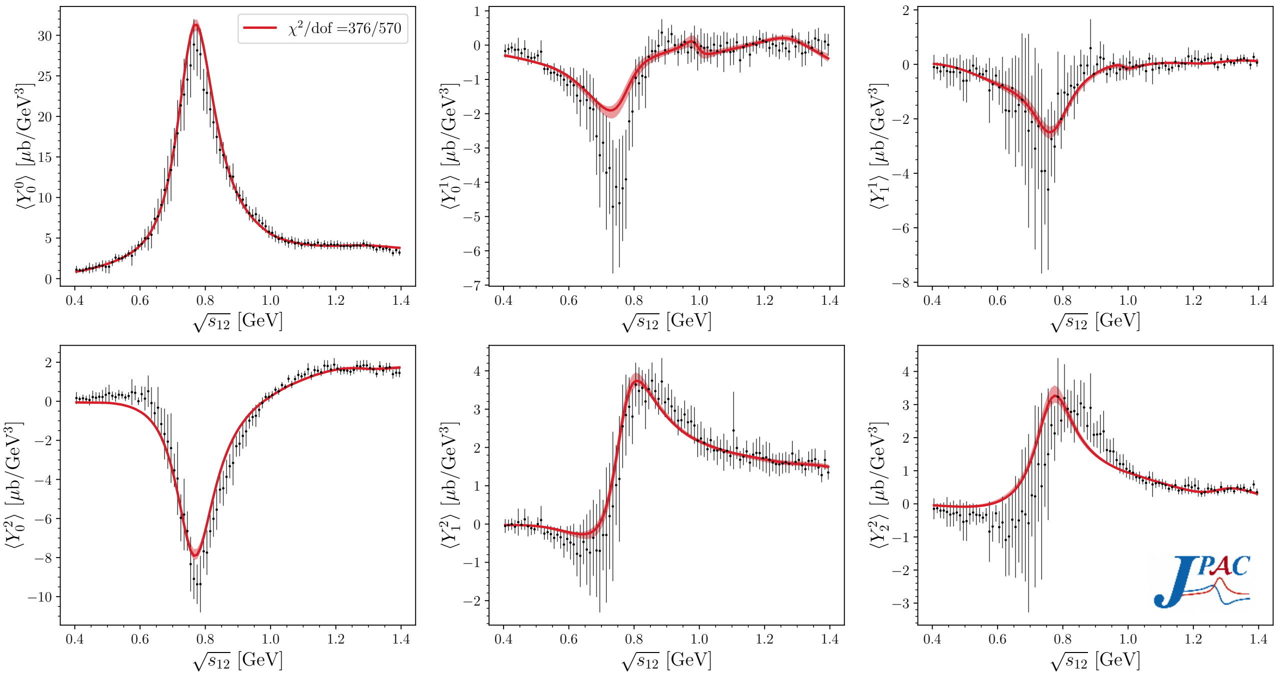

Figure 1: Comparison of the complete model fitted to experimental measurements from Ref. [13] of two-pion angular moments $\langle Y^L_M \rangle$ for $L = 0, 1, 2$ and $M = 0, \ldots, L$ at $E_\gamma = 3.7$ GeV and $t = -0.45$ GeV^2.

[7] A. Donnachie and P. V. Landshoff. Total cross-sections. *Phys. Lett. B*, 296:227–232, 1992.

[8] Battaglieri et al. Photoproduction of the ρ^0 meson on the proton at large momentum transfer. *Phys. Rev. Lett.*, 87:172002, Oct 2001.

[9] S. Adhikari et al. Measurement of spin-density matrix elements in $\rho(770)$ production with a linearly polarized photon beam at Eγ=8.2–8.8 GeV. *Phys. Rev. C*, 108(5):055204, 2023.

[10] Ł. Bibrzycki, P. Bydžovský, R. Kamiński, and A. P. Szczepaniak. Meson resonances in forward-angle $\pi^+\pi^-$ photoproduction. *Phys. Lett. B*, 789:287–291, 2019.

[11] Nadine Hammoud. Studying light flavour resonances with polarised photon beams. *PoS*, ICHEP2022:837, 2022.

[12] Miguel Albaladejo et al. Novel approaches in hadron spectroscopy. *Prog. Part. Nucl. Phys.*, 127:103981, 2022.

[13] M. Battaglieri et al. Photoproduction of pi+ pi- meson pairs on the proton. *Phys. Rev. D*, 80:072005, 2009.